



## Effect of chia mucilage addition on oxidation and release kinetics of lemon essential oil microencapsulated using mesquite gum – Chia mucilage mixtures



Stefani Cortés-Camargo<sup>a</sup>, Pedro Estanislao Acuña-Avila<sup>b</sup>, María Eva Rodríguez-Huezo<sup>c</sup>,  
Angélica Román-Guerrero<sup>d</sup>, Victor Varela-Guerrero<sup>e</sup>, César Pérez-Alonso<sup>a,\*</sup>

<sup>a</sup> Facultad de Química, Universidad Autónoma del Estado de México, Paseo Colón esq. Paseo Toluca s/n, Col. Residencial Colón, Toluca, Estado de México 50120, Mexico

<sup>b</sup> Universidad Tecnológica de Zinacantepec, Av. Libramiento Universidad 106, Col. San Bartolo el Llano, Zinacantepec, Estado de México 51361, Mexico

<sup>c</sup> Tecnológico de Estudios Superiores de Ecatepec, Departamento de Ingeniería Química y Bioquímica, Av. Tecnológico s/n esq. Av. Central, Col. Valle de Anáhuac, Ecatepec, Estado de México 55210, Mexico

<sup>d</sup> Departamento de Biotecnología, Universidad Autónoma Metropolitana-Iztapalapa, San Rafael Atlixco 186, Col. Vicentina, Ciudad de México 09340, Mexico

<sup>e</sup> Centro Conjunto de Investigación en Química Sustentable UAEM - UNAM, Carretera Toluca-Atacomulco, km 14.5, Unidad El Rosedal, Toluca, Estado de México 50200, Mexico

### ARTICLE INFO

#### Keywords:

Chia mucilage  
Mesquite gum  
Lemon essential oil  
Microencapsulation  
Oil oxidation kinetics  
Oil release kinetics

### ABSTRACT

Lemon essential oil (LEO) emulsions were prepared using mesquite gum (MG) - chia mucilage (CM) mixtures (90-10 and 80-20 MG-CM weight ratios) and MG as control sample, LEO emulsions were thenspray dried for obtaining the respective microcapsules. LEO emulsions were analyzed by mean droplet size and apparent viscosity, while microcapsules were characterized through mean particle size, morphology, volatile oil retention ( $\leq 51.5\%$ ), encapsulation efficiency ( $\geq 96.9\%$ ), as well as oxidation and release kinetics of LEO. The LEO oxidation kinetics showed that 90-10 and 80-20 MG-CM microcapsules displayed maximum peroxide values of 91.6 and 90.5 meq hydroperoxides  $\text{kg}^{-1}$  of oil, respectively, without significant differences between them ( $p > .05$ ). MG-CM microcapsules provided better protection to LEO against oxidation than those formed with MG; where the oxidation kinetics were well adjusted to zero-order ( $r^2 \geq 0.94$ ). The LEO release kinetics from microcapsules were carried out at different pH (2.5 and 6.5) and temperature (37 °C and 65 °C) and four mathematical models (zero-order, first-order, Higuchi and Peppas) were used to evaluate the experimental data; the release kinetics indicated that the 80-20 MG-CM microcapsules had a longer delay in LEO release rate, followed by 90-10 MG-CM and MG microcapsules, hence, CM addition in MG-CM microcapsules contributed to delay the LEO release rate. This work clearly demonstrates that use of a relatively small amount of CM mixed with MG improves oxidative stability and delays the release rate of encapsulated LEO regarding MG microcapsules, therefore, MG-CM mixtures are interesting additives systems suitable for being applied in food industry.

### 1. Introduction

Mucilages are functional biopolymers commonly extracted from plants (seeds or soft stems) that are easily obtained by soaking in water (Kaewmanee et al., 2014). They have functional properties such as water binding, texture modifier, gelling, emulsifying, foaming and encapsulating agents and have been applied in formulations of coacervates (Timilsena, Adhikari, Barrow, & Adhikari, 2016), emulsions and edible films (Dick et al., 2015) and as wall materials in active

compounds microencapsulation (De Campo et al., 2017), thus, mucilages represent interesting alternatives of additives for food industry.

Chia mucilage (CM) is a tetrasaccharide with 4-*O*-methyl- $\alpha$ -D-glucopyranosyl residues occurring as branches of  $\beta$ -D-xylopyranosyl residues in the main chain consisting of (1  $\rightarrow$  4)- $\beta$ -D-xylopyranosyl-(1  $\rightarrow$  4)- $\alpha$ -D-glucopyranosyl-(1  $\rightarrow$  4)- $\beta$ -D-xylopyranosyl units. Acid hydrolysis yields  $\beta$ -D-xylose,  $\alpha$ -D-glucose and 4-*O*-methyl- $\alpha$ -D-glucuronic acid in 2:1:1 proportion. The average molecular weight of CM ranges from 0.8 to  $2 \times 10^6$  Da (Lin, Daniel, & Whistler, 1994). A proximal

\* Corresponding author.

E-mail address: [cpereza@uaemex.mx](mailto:cpereza@uaemex.mx) (C. Pérez-Alonso).

<https://doi.org/10.1016/j.foodres.2018.09.040>

Received 20 December 2017; Received in revised form 5 September 2018; Accepted 15 September 2018

Available online 20 September 2018

0963-9969/ © 2018 Elsevier Ltd. All rights reserved.

analysis of CM powder reveals that it is constituted by carbohydrates ( $63.7 \pm 0.5$ ), crude fiber ( $13.5 \pm 0.6$ ), protein ( $11.2 \pm 0.3$ ), moisture ( $11.5 \pm 0.3$ ), ashes ( $8.4 \pm 0.1$ ) and lipids ( $3.1 \pm 0.2$ ) expressed as g/100 g (Capitani, Ixtaina, Nolasco, & Tomás, 2013). The high protein content of CM favors its emulsifying properties, while its high carbohydrates and fiber contents favor its encapsulating properties since it tends to form gels (De Campo et al., 2017). CM has an adequate oil holding capacity, which is useful for oil-based active compounds retention (Segura-Campos, Ciau-Solís, Rosado-Rubio, Chel-Guerrero, & Betancur-Ancona, 2014). CM has a high water holding capacity (23 g of water /g of mucilage) similar to guar gum, high viscosity values at low concentrations (Timilsena, Adhikari, Kasapis, & Adhikari, 2016) and gelling properties so it could be used as texture modifier (Goh et al., 2016). In addition, a study of CM thermodynamic properties demonstrated that it could be used as wall material in spray drying microencapsulation (Velázquez-Gutiérrez et al., 2015). CM has been applied in edible films formulation blended with proteins (Capitani et al., 2016), in emulsions stabilization (Guiotto, Capitani, Nolasco, & Tomás, 2016), in the microencapsulation by spray drying using co-encapsulates complexes (Timilsena, Adhikari, Barrow, et al., 2016), and in the nanoencapsulation by freeze drying (De Campo et al., 2017).

On the other hand, mesquite gum (MG) is an exudate from *Prosopis* spp. trees that is formed by a highly branched complex heteropolyelectrolyte that upon hydrolysis with dilute mineral acid yields L-arabinose,  $\beta$ -D-galactose, and 4-O-methyl-D-glucuronic acid in a molar ratio of 4:2:1 and it has an average molecular weight of  $2.12 \times 10^6$  Da (Vernon-Carter, Beristain, & Pedroza-Islas, 2000). MG has been applied as emulsifying and encapsulating agent in spray drying (Escalona-García et al., 2016; Fuentes-Ortega et al., 2017).

There is a tendency to mix biopolymers for improving their individual characteristics in the retention and protection of microencapsulated active compounds obtained by spray drying. In this case, novel MG-CM mixtures are proposed for lemon essential oil (LEO) microencapsulation, an oil highly applied in the food industry but with oxidation problems. It should be noted that CM has not been studied as an encapsulating agent in spray drying since at high concentrations it produces emulsions with extremely high apparent viscosity values; for that reason CM was mixed with MG, since MG can be used at very high concentrations maintaining relatively low viscosity values (Vernon-Carter et al., 1996).

Therefore, the aim of this work was to determine the effect of CM addition using MG-CM mixtures as wall materials in the LEO microencapsulation, on characteristics such as the retention, protection against oxidation and release rate of microencapsulated oil through the analysis of volatile oil retention, encapsulation efficiency, as well as, by an oxidation kinetic per peroxide value and a release kinetic in aqueous medium of the microencapsulated oil.

## 2. Materials and methods

### 2.1. Materials

Chia (*Salvia hispanica* L.) seeds were obtained from local farmers from Atlxco region in the state of Puebla, Mexico. Mesquite gum (MG) was obtained from *Prosopis laevigata* trees in San Luis Potosí, Mexico. The gum was collected as an exudate from trees and it was pulverized, purified and spray-dried according to Vernon-Carter et al. (1996). Lemon essential oil (LEO) was purchased from Droguería Cosmopolita, S.A. de C.V., Mexico City, Mexico. Distilled and deionized water were used in the experiments. All chemical reagents were purchased from Sigma-Aldrich S.A. de C.V. (Toluca, State of Mexico, Mexico).

### 2.2. Chia mucilage extraction

CM was extracted from the seeds using the method of Muñoz, Cobos, Diaz, and Aguilera (2012). Briefly, samples of 110 g of the whole

seeds were placed in a 3.5 L stainless steel container and distilled water was added in 1:20 seeds-water ratio and pH value was adjusted to 8.0 using 1 N NaOH solution. The mixture was hydrated at 86 °C for 2 h under stirring with a stirrer model BDC-3030 (Caframo, Ontario, Canada). Thereafter, the aqueous suspension was spread on a drying tray and exposed to temperature of 65 °C for 2.5 h in an air convection heat oven model HCX II (San-son plus, State of Mexico, Mexico). The dried mucilage was separated from the seed by rubbing over a 40 mesh screen.

### 2.3. Emulsions preparation

Oil-in-water (o/w) emulsions were prepared using MG-CM mixtures in 90–10 and 80–20 ratios, and MG as the control. Briefly, aqueous dispersions of biopolymers at 20% (w/w) were supplemented with 0.02% (w/v) of sodium azide to prevent microorganisms' growth and were adjusted to pH = 7.0 using 1 N NaOH solution. Emulsions were formulated using a core to wall material (Co:Wa) ratio of 1:3 and a total solids content of 26.6%. Emulsification process was carried out using an Ultra-Turrax T50 homogenizer (IKA®-Werke Works Inc., Wilmington, NC, USA) at 6400 rpm during 5 min (Cortés-Camargo et al., 2017) maintaining the temperature below 30 °C with an ice bath. The emulsions were stored in closed amber glass bottles at 4 °C, for 24 h until their analysis.

### 2.4. Emulsions characterization

#### 2.4.1. Droplet size distribution

The mean droplet diameter of the emulsions was determined by laser diffraction using a Malvern Mastersizer 2000 (Malvern Instruments Ltd., Worcestershire, UK). The refractive index of emulsions was 1.364 and the obscuration was in a range of 15–20%. Volume-weighted mean diameter ( $D[4,3]$ ), area-volume mean diameter or Sauter diameter ( $D[3,2]$ ) and "span" parameter (distribution width of droplet size) were obtained (García, Alfaro, Calero, & Muñoz, 2014).

#### 2.4.2. Apparent viscosity

Apparent viscosity of the emulsions was measured using a Physica MCR300 Rheometer (Physica Messtechnik GmbH, Stuttgart, Germany). Different geometry was used according to the type of emulsion, i.e. MG-CM emulsions were analyzed using a stainless steel cone-plate geometry with a rotating cone of 50 mm in diameter and cone angle of 2° with a gap of 0.2 mm, while MG emulsion was measured using double-gap geometry (DG 26.7) due to its low viscosity value. Samples of ~1.25 mL were carefully placed in the measuring system, and were left at rest for 5 min at 25 °C for structure recovery. Viscosity curves of the emulsions were obtained by increasing the shear rate ( $\dot{\gamma}$ ) from 0.001 to 1000 s<sup>-1</sup> in 5 min at 25 °C (Utrilla-Coello et al., 2014). The viscosity curves of MG-CM emulsions were adjusted to Cross (Cross, 1965) model:

$$\eta_a = \eta_\infty + \frac{(\eta_0 - \eta_\infty)}{[1 + (\lambda\dot{\gamma})^m]} \quad (1)$$

where  $\dot{\gamma}$  is the shear rate (s<sup>-1</sup>),  $\eta_a$  is the apparent viscosity (Pa s),  $\eta_0$  is the zero-shear rate viscosity (Pa s),  $\eta_\infty$  is the infinite shear rate viscosity (Pa s),  $\lambda$  is the relaxation time (s), and  $m$  is a dimensionless constant related to the power law exponent (Sittikijyothin, Torres, & Gonçalves, 2005). The viscosity curve of MG emulsion was fitted to the Power Law model:

$$\eta_a = K\dot{\gamma}^{(n-1)} \quad (2)$$

where  $K$  is the consistency index (Pa s <sup>$n$</sup> ) and  $n$  is the power law exponent or flow index (dimensionless) (Steffe, 1996).

## 2.5. Microencapsulation by spray drying

Emulsions were prepared and immediately dried using a Nichols/Niro spray-drier (Turbo Spray PLA, NY, USA) with a feed rate of  $5 \text{ mL min}^{-1}$  and, inlet and outlet air temperatures of  $135 \pm 5^\circ\text{C}$ , and  $80 \pm 5^\circ\text{C}$  respectively, with an atomization pressure of 4 bar (Cortés-Camargo et al., 2017). The microcapsules were collected and stored in sealed polyethylene bags, wrapped with aluminum foil, and were introduced to a desiccator ( $20^\circ\text{C}$ ) until their analysis.

## 2.6. Microcapsules characterization

### 2.6.1. Moisture content

The initial moisture content of the microcapsules was measured gravimetrically by vacuum oven drying at  $70^\circ\text{C}$  and  $< 7 \text{ kPa}$  until reach constant weight (Bringas-Lantigua, Expósito-Molina, Reineccius, López-Hernández, & Pino, 2011).

### 2.6.2. Particle size distribution

The volume-weighted mean diameter ( $D[4,3]$ ) of the microcapsules was measured using a particle size analyzer Malvern Mastersizer 2000 (Malvern Instruments Ltd., Malvern, Worcestershire, UK). Microcapsules were dispersed in 2-propanol with a refractive index of 1.385, an adsorption index of 0.1 and an air pressure of 4 bar (Rodea-González et al., 2012).

### 2.6.3. Scanning electron microscopy

Microcapsules morphology was observed using a scanning electron microscope (SEM) model JSM-6510LV (Jeol Co. Ltd., Tokyo, Japan) at an accelerating voltage of 15 kV. The samples were placed on the SEM stubs using a double-sided sticky tape (Ted Pella, Redding, California, USA) and subsequently coated with gold using sputtering at 100 millitorrs and 15 mA (Denton Vacuum Model, USA) (Rodea-González et al., 2012).

### 2.6.4. Total volatile oil retention

Total volatile oil retention of the microcapsules was determined using Clevenger distillation according to the method reported by Bringas-Lantigua et al. (2011) with slight modifications. 7.5 g of microcapsules were dissolved in 100 mL of distilled water at  $20^\circ\text{C}$  and the dispersion was poured into a 250 mL round-bottom flask. The distillation was carried out under constant stirring for 1.5 h, and the volume of distilled oil was directly read in the scale of the collection arm. Volatile oil retention (%VOR) was calculated dividing total volatile oil (TVO) measured in the collection arm over theoretical oil content (TOC) and expressed as percentage. The density of LEO was of  $0.87 \text{ g mL}^{-1}$  at  $20^\circ\text{C}$ , measured with a DMA 35 density meter (Anton Paar GmbH, Graz, Austria).

### 2.6.5. Encapsulation efficiency

The encapsulation efficiency was determined using the method of Bringas-Lantigua et al. (2011) with slight modifications. At first, the surface LEO of the microcapsules, i.e. LEO that was not entrapped within the microcapsule core, was extracted by adding 7.5 g of microcapsules into 20 mL of hexane solvent and gently shaken for 20 min, the resultant dispersion was filtered through a Whatman filter paper grade 1. The microcapsules collected on the filter were rinsed three times using 10 mL of hexane each time, then the residual solvent of the microcapsules was evaporated at  $20^\circ\text{C}$  until reach constant weight.

The resultant microcapsules, with no oil on their surfaces, were weighed and dissolved in 100 mL of distilled water in order to determine their LEO core content by means of Clevenger distillation. The surface LEO content (SO) of microcapsules was calculated by mass difference between the retained total volatile oil (TVO) obtained in Section 2.6.4, and the core LEO content obtained in this section. The encapsulation efficiency (EE) was calculated using the Eq. (3) (Carneiro,

Tonon, Grosso, & Hubinger, 2013):

$$EE = \frac{TVO - SO}{TVO} \times 100 \quad (3)$$

### 2.6.6. Oil oxidation by peroxide value

The oil oxidation was evaluated by peroxide value method at time zero (right after drying) and over seven weeks of storage. The conditioning was carried out by placing 0.5 g of microcapsules inside a glass vial (20 mL) and these were stored at  $35^\circ\text{C}$  in order to accelerate the oxidation process with a controlled water activity ranging from 0.16 to 0.35.

The peroxide value was performed according to the method of Shantha and Decker (1994) with slight modifications. Briefly, 0.5 g of microcapsules were dispersed in 1.0 mL of distilled water, 0.3 mL of the reconstituted emulsion were mixed with 1.5 mL of isoctanol/iso-propanol 3:2 (v/v), and vortexed three times for 10 s using a Vortex 3 Orbital Shakers (IKA, Germany). The samples were centrifuged using a 5810 R centrifuge (Eppendorf, Hamburg, Germany) at  $3150 \times g$  for 10 min. 0.2 mL of the upper organic layer were added to 2.8 mL of methanol/1-butanol solution 2:1 (v/v), followed by adding 15  $\mu\text{L}$  of 3.94 M ammonium thiocyanate and 15  $\mu\text{L}$  of ferrous iron solution. The ferrous iron solution was the supernatant of a mixture of 25 mL  $\text{BaCl}_2$  solution (0.132 M  $\text{BaCl}_2$  in 0.4 M HCl) and 25 mL of 0.144 M  $\text{FeSO}_4$  solution. The absorbance was read at 510 nm after 20 min, using a UV/Vis spectrophotometer model Genesys 10 (Thermo Scientific, Waltham, MA, USA) and the hydroperoxides concentrations were calculated using a standard curve of cumene hydroperoxides (Niu et al., 2016).

**2.6.6.1. Oil oxidation kinetics.** Peroxide value-time curves of LEO and encapsulated LEO were fitted to zero and first order using linear Eqs. (4) and (5), respectively (Labuza, 1984):

$$C_{HP} = K_{HP}t + C_{HP0} \quad (4)$$

$$\ln C_{HP} = \ln C_{HP0} + K_{HP}t \quad (5)$$

where  $C_{HP0}$  is the initial peroxide value at time 0 (right after drying),  $C_{HP}$  is the peroxide value after  $t$  (time),  $K_{HP}$  is the hydroperoxides formation rate constant which was obtained from the slope of the peroxide value-time curve, in this case  $K_{HP}$  had positive sign since hydroperoxides formation increased over time (Escalona-García et al., 2016).

### 2.6.7. Oil release kinetics

Release kinetics of LEO from microcapsules was carried out using the method described by Dima, Pătrașcu, Cantaragiu, Alexe, and Ștefan (2016) with slight modifications. Phosphate buffer solution (PBS) at pH values of 2.5 and 6.5 were prepared and mixed with ethanol in a 3:2 ratio (v/v). 0.75 g of LEO microcapsules were added in an Erlenmeyer flask containing 60 mL PBS - ethanol solution and it was slowly stirred at constant temperature ( $37^\circ\text{C}$  and  $65^\circ\text{C}$ ). Samples of 2 mL were sucked out for analysis at specific time intervals, and immediately replaced with 2 mL of fresh media (PBS - ethanol solution). The samples were centrifuged using a 5810 R centrifuge (Eppendorf, Hamburg, Germany) at  $3150 \times g$  for 10 min at  $25^\circ\text{C}$  and the supernatants were used to determine the LEO concentration with a UV-VIS spectrophotometer model Genesys 10 (Thermo Scientific, Waltham, MA, USA) at a wavelength of 273 nm, using as blank sample PBS - ethanol 3:2 (v/v) solution. The LEO concentration in the release medium at sampling time intervals was calculated using a calibration curve of LEO in PBS - ethanol 3:2 (v/v) solution (Absorbance =  $0.2765(\text{LEO conc. (mg/mL)}) + 0.3618$ ;  $r^2 = 0.99$ ). The cumulative percentage (Q) of released LEO was obtained using the Eq. (6):

$$Q = \sum_{t=0}^t \frac{M_t}{M_0} \times 100 \quad (6)$$

**Table 1**

Parameters of droplet size distribution of LEO emulsions stabilized with MG-CM mixtures and MG.

	D[4,3] $\mu\text{m}$	D[3,2] $\mu\text{m}$	Span
90-10 MG-CM	36.88 $\pm$ 0.64 <sup>a</sup>	1.84 $\pm$ 0.00 <sup>a</sup>	61.95 $\pm$ 1.23 <sup>a</sup>
80-20 MG-CM	48.60 $\pm$ 6.73 <sup>a</sup>	1.94 $\pm$ 0.09 <sup>a</sup>	66.83 $\pm$ 3.21 <sup>a</sup>
MG	1.46 $\pm$ 0.01 <sup>b</sup>	1.10 $\pm$ 0.01 <sup>b</sup>	0.92 $\pm$ 0.00 <sup>b</sup>

Data are presented as means  $\pm$  SD ( $n = 3$ ).

Values with different letters in the same column indicate significant difference ( $p \leq .05$ ).

LEO: lemon essential oil; MG: mesquite gum; CM: chia mucilage; D[4,3]: volume-weighted mean diameter; D[3,2]: area-volume mean diameter or Sauter diameter.

where  $M_t$  is the cumulative amount of LEO released in the medium at each sampling time and  $M_0$  is the initial mass of LEO loaded in the sample.

### 2.7. Statistical analysis

Statistical analysis was performed in triplicate for each sample for all the tests, and data are shown as means  $\pm$  standard deviation. Data were analyzed using a one way analysis of variance (ANOVA) and Tukey's test at a significance level  $p \leq .05$  using Minitab version 16.0 software (Minitab Inc., State College, PA, USA).

## 3. Results and discussion

### 3.1. Emulsions characterization

#### 3.1.1. Droplet size distribution and apparent viscosity

Table 1 shows the parameters of droplet size distribution of LEO emulsions stabilized with MG-CM mixtures and MG. The volume-weighted mean diameter D[4,3] and Sauter diameter D[3,2], of 90–10 and 80–20 MG-CM emulsions were significantly ( $p \leq .05$ ) larger than those of MG emulsion, but showed no significant difference ( $p > .05$ ) between them. The larger droplet mean sizes of MG-CM mixtures can be attributed to certain characteristics of CM, such as high water holding capacity and high viscosity of the mucilage (Timilsena, Adhikari, Kasapis, et al., 2016). In contrast, MG emulsion had very small mean droplet size due to the compact structure, high solubility in water and low viscosity of MG (Vernon-Carter et al., 2000), which allows a very rapid diffusion and anchoring of MG molecules to the oil-water interface. Therefore, structural and functional differences between both biopolymers lead to significant differences in their droplet mean diameters. The width of the droplet size distribution or “span” (Table 1) values indicate that MG-CM emulsions had high polydispersity, i.e. heterogeneous droplet size distribution, while MG emulsion was predominantly monodisperse, i.e. it had a homogeneous size distribution. Fig. 1 shows that MG-CM emulsions showed a bimodal behavior, while MG emulsion a unimodal behavior characterized by basically a peak corresponding to its predominant size. Piorkowski and McClements (2014) have determined that homogeneous systems with narrow unimodal distribution display higher emulsion stability over the time; although emulsion stability may also depend on other factors.

Fig. 2 shows apparent viscosity ( $\eta_a$ ) of LEO emulsions at 26.6% of total solids. MG-CM emulsions had higher  $\eta_a$  values than MG emulsion and as CM concentration in MG-CM emulsions increased, the  $\eta_a$  also increased. 80–20 MG-CM emulsion had the highest  $\eta_a$  (14.86 Pa s at  $\dot{\gamma} = 0.005 \text{ s}^{-1}$ ) and was able to flow without tendency to form a weak gel. The high viscosity of CM is related with its content of 4-O-methyl glucuronic acid that forms intermolecular bonds in aqueous medium (Timilsena, Adhikari, Kasapis, et al., 2016) which lead to higher water retention and molecular swelling. The viscosity curves of MG-CM emulsions (Fig. 2) showed three well-defined regions: (1) Newtonian-Plateau region where the viscosity

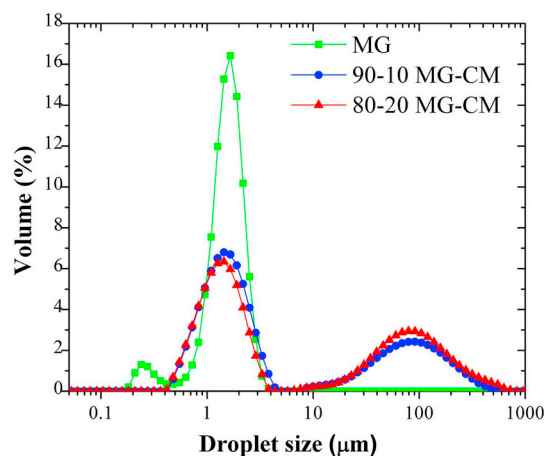


Fig. 1. Droplet size distribution of lemon essential oil emulsions stabilized with mesquite gum – chia mucilage (MG-CM) mixtures and MG stored for 24 h, 25 °C. Average values are shown ( $n = 3$ ).

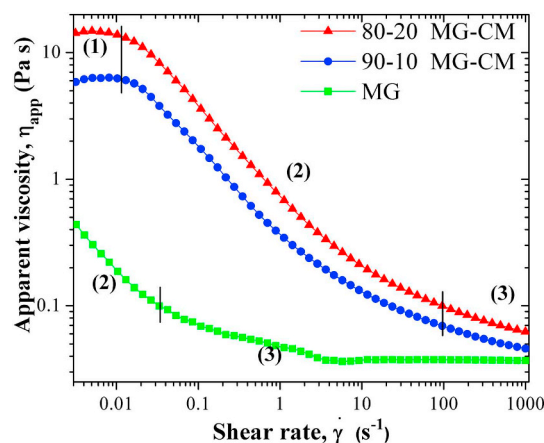


Fig. 2. Apparent viscosity-shear rate behavior of lemon essential oil emulsions stabilized with mesquite gum – chia mucilage (MG-CM) mixtures and MG at 25 °C. (1) Newtonian-Plateau region; (2) Shear-thinning or pseudoplastic region; (3) infinite viscosity region. Average values are shown ( $n = 3$ ).

has a constant value at lower shear rates, (2) shear-thinning or pseudoplastic region where the viscosity decreases with increasing shear rate and (3) the infinite shear viscosity region at higher shear rates (García et al., 2014; Sittikijyothin et al., 2005). On the other hand, the viscosity curve of MG emulsion only had two well-defined regions, the pseudoplastic and infinite shear viscosity region. The viscosity curves of MG-CM emulsions were well fitted to Cross model ( $r^2 \geq 0.99$ ) (Table 2). As concentration of CM in MG-CM emulsions increased, the relaxation times ( $\lambda$ ) also increased due to the increase in  $\eta_a$  and reduction of molecular movement by greater cross-linking (Lopes da Silva, Gonçalves, & Rao, 1992). The structure of 80–20 MG-CM emulsion had the greatest resistance to viscosity drop when increasing the shear rate, since it took more time to move from the Newtonian-Plateau region to pseudoplastic region. The “ $m$ ” parameter of Cross model allowed to determine the fluids pseudoplasticity (Cervantes-Martínez et al., 2014), MG-CM emulsions had “ $m$ ” values close to or greater than one and were classified as non-Newtonian fluids of pseudoplastic type. Cross model has been used to represent the rheological behavior of viscosity curves of mucilages obtained from *Aloe vera* (Cervantes-Martínez et al., 2014) and *pitahaya* (*Hylocereus undatus*) (García-Cruz, Rodríguez-Ramírez, Méndez-Lagunas, & Medina-Torres, 2013). The viscosity curve of MG emulsion (Fig. 2) was adjusted to Power Law model ( $r^2 = 0.98$ ) and its  $\eta_a$  values dropped rapidly due to alignment of its molecules to the shear field, reaching infinite viscosity values at low shear rates. Viscosity and droplet size of emulsions are directly related. High

**Table 2**  
Parameters of cross model of LEO emulsions stabilized with MG-CM mixtures.

Cross	$\eta_o$ (Pa s)	$\eta_\infty$ (Pa s)	$\lambda$ (s)	$m$	$r^2$
90-10 MG-CM	6.73 ± 0.12 <sup>b</sup>	0.14 ± 0.03 <sup>a</sup>	22.30 ± 1.07 <sup>a</sup>	1.33 ± 0.07 <sup>a</sup>	0.99
80-20 MG-CM	15.96 ± 0.23 <sup>a</sup>	0.23 ± 0.05 <sup>a</sup>	26.36 ± 1.00 <sup>a</sup>	1.24 ± 0.04 <sup>a</sup>	1.00

Data are presented as means ± SD (n = 3).

Values with different letters in the same column indicate significant difference ( $p \leq .05$ ).

LEO: lemon essential oil; MG: mesquite gum; CM: chia mucilage;  $\eta_o$ : zero-shear rate viscosity;  $\eta_\infty$ : infinite-shear rate viscosity;  $\lambda$ : relaxation time;  $m$  is a dimensionless constant;  $r^2$ : coefficient of linear determination.

viscosity emulsions slow down the diffusion of biopolymers molecules to the interface during homogenization, resulting in larger oil droplet sizes (Piorkowski & McClements, 2014). In this case, MG-CM emulsions had higher viscosity, larger droplet sizes and higher heterogeneity than that of the MG.

### 3.2. Microcapsules characterization

#### 3.2.1. Moisture content, particle size distribution and morphology

Table 3 shows the moisture content and volume-weighted mean diameter  $D[4,3]$  of the LEO microcapsules. The moisture content ranged from 2.17 to 3.89%. MG-CM microcapsules had larger  $D[4,3]$  than MG microcapsules, and the three microcapsules systems showed significant difference between them ( $p \leq .05$ ). As concentration of CM in MG-CM microcapsules increased,  $D[4,3]$  also increased. Particle mean diameter of microcapsules is related with droplet mean diameter of inlet emulsions, i.e., microcapsules with larger particle size were obtained from emulsions with larger droplet size and higher viscosity (Carneiro et al., 2013). It should be noted that MG-CM microcapsules did not show tendency to the agglomeration. Fig. 3 shows the particle size distribution of LEO microcapsules where the three microcapsules systems had a bimodal behavior with heterogeneous particle sizes or high polydispersity, however, MG-CM microcapsules showed greater amplitude in the particle size distribution than those of MG.

Fig. 4 shows micrographs obtained by scanning electron microscopy of LEO microcapsules. Fig. 4a–c correspond to 90-10 MG-CM, 80-20 MG-CM, and MG microcapsules, respectively. MG microcapsules were smaller sized than the MG-CM microcapsules, whose particle size increased as CM concentration augmented in MG-CM mixtures. All the microcapsules were characterized for displaying irregular spheres shapes with wrinkled surfaces. Shrinkage phenomenon during spray drying is influenced by variables such as drying conditions, inlet emulsion viscosity and wall material characteristics (Jafari, Assadpoor, He, & Bhandari, 2008). In this work, the three microcapsules systems were obtained under the same conditions, so MG microcapsules shrinkage was associated with a rapid spray drying rate since its emulsion had low viscosity values which allowed a rapid flow to the drier interior (Cortés-Camargo et al., 2017), while MG-CM microcapsules shrinkage was attributed to the scarce flexibility and resistance of the wall materials (Tan, Chan, & Heng, 2009). Addition of CM in MG-CM emulsions increased their viscosity, which delayed the drying process, but it was not enough to avoid shrinkage.

**Table 3**  
Characterization of LEO microcapsules covered with MG-CM mixtures and MG.

	Moisture content (%)	$D[4,3]$ ( $\mu\text{m}$ )	Volatile oil retention (%)	Encapsulation efficiency (%)
90-10 MG-CM	3.89 ± 0.06 <sup>a</sup>	13.80 ± 0.24 <sup>b</sup>	49.6 ± 1.9 <sup>a</sup>	98.3 ± 1.4 <sup>a</sup>
80-20 MG-CM	3.23 ± 0.02 <sup>b</sup>	18.38 ± 0.45 <sup>a</sup>	51.5 ± 1.7 <sup>a</sup>	98.6 ± 1.3 <sup>a</sup>
MG	2.17 ± 0.14 <sup>c</sup>	9.81 ± 0.12 <sup>c</sup>	42.0 ± 1.0 <sup>b</sup>	96.9 ± 1.7 <sup>a</sup>

Data are presented as means ± SD (n = 3).

Values with different letters in the same column indicate significant difference ( $p \leq .05$ ).

LEO: lemon essential oil; MG: mesquite gum; CM: chia mucilage;  $D[4,3]$ : volume-weighted mean diameter.

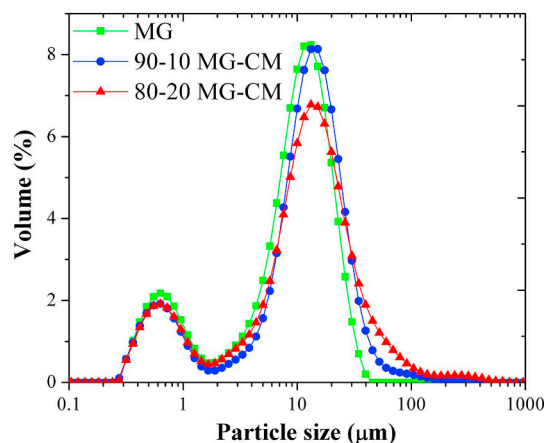


**Fig. 3.** Particle size distribution of lemon essential oil microcapsules covered with mesquite gum – chia mucilage (MG-CM) mixtures and MG. Average values are shown (n = 3).

#### 3.2.2. Volatile oil retention and encapsulation efficiency

Table 3 shows the total volatile oil retention (VOR) of LEO microcapsules. The three microcapsules systems had a content of VOR  $\leq 51.5\%$ . 90–10 and 80–20 MG-CM microcapsules had higher VOR than MG microcapsules, and these mixtures showed no significant differences ( $p > .05$ ) between them. The VOR values of MG-CM microcapsules were mainly associated with the inlet emulsions characteristics which presented larger droplet sizes and higher viscosity values, thus, MG-CM emulsions took longer to form the film around the large droplets during spray drying and consequently, they suffered a great loss of volatile compounds (Soottitantawat et al., 2005). Cortés-Camargo et al. (2017) reported VOR values in a range of 58.2–70.3% for LEO microcapsules covered with MG-nopal mucilage mixtures.

Table 3 shows encapsulation efficiency (EE) of LEO microcapsules. All the microcapsules systems had no significant difference ( $p > .05$ ) in their EE values ( $\geq 96.9\%$ ). High EE values indicate a greater protection of oil against oxidation since most of the oil is inside of the microcapsule. High EE values of MG-CM microcapsules can be related to the high viscosity of the inlet emulsions which avoid oil droplet migration towards the particle surface (Tonon, Grosso, & Hubinger, 2011), and also to the enhanced film-forming capacity by CM in MG-CM mixtures.

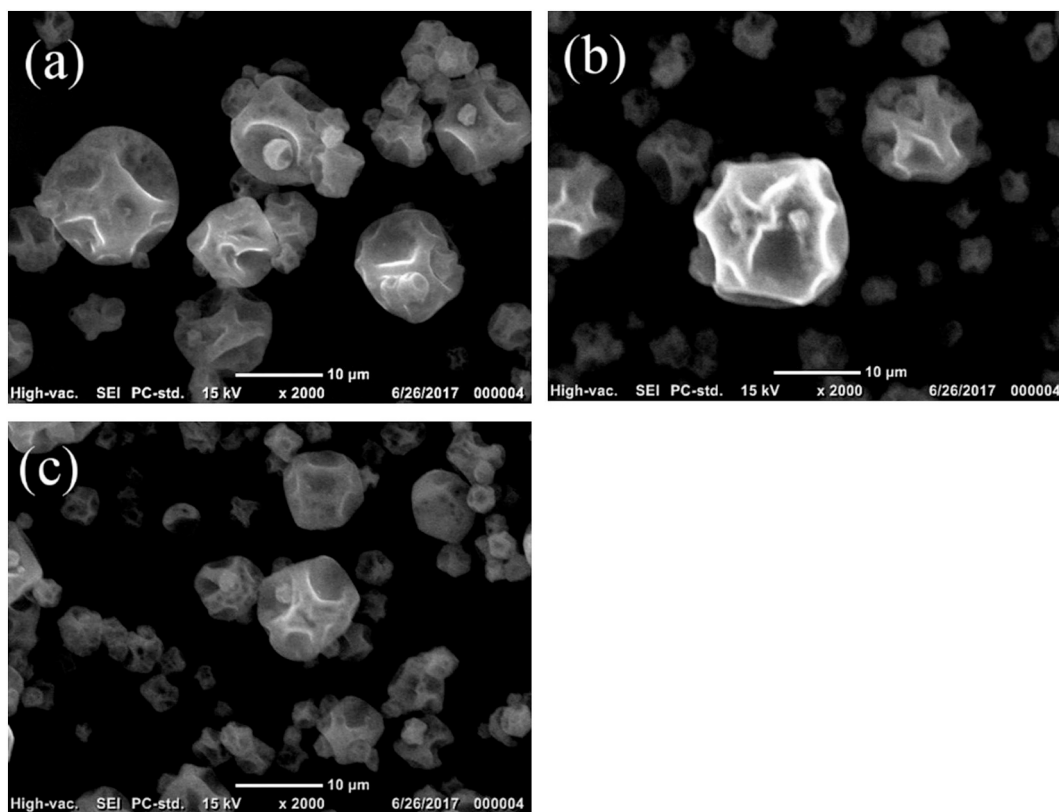


Fig. 4. Micrographs of lemon essential oil microcapsules covered with mesquite gum – chia mucilage mixtures (a) 90–10 MG-CM, (b) 80–20 MG-CM and (c) MG, at 10 µm scale.

which protect the emulsion from extensive oil droplet disruption during atomization process by spray drying (Tonon, Pedro, Grosso, & Hubinger, 2012). Timilsena, Adhikari, Barrow, et al. (2016) used chia seed gum at very low concentration (2.6 g of gum / 500 mL of water) for micro-encapsulating chia seed oil by spray drying with an EE value of  $63.1 \pm 1.9\%$ , however, when chia seed gum - chia seed protein isolate complex coacervates were used, the EE values increased up to  $93.9 \pm 4.6\%$ .

In the case of MG microcapsules, their high EE value can be attributed to their emulsion characteristics such as small particle sizes, low viscosity values and consequently, high emulsion stability. Some studies have shown higher EE values of the oils and flavorings, by decreasing the droplet size and increasing emulsion stability (Carneiro et al., 2013; Tonon et al., 2012).

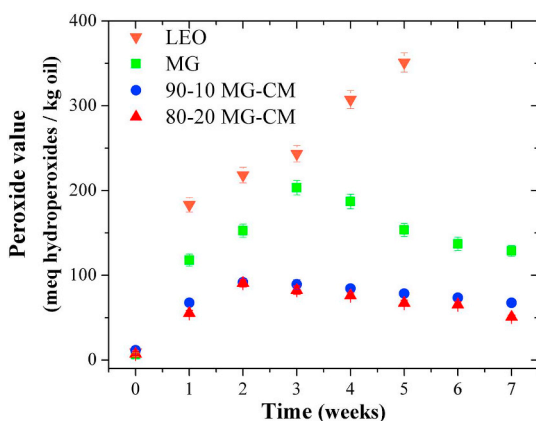


Fig. 5. Oxidation kinetic of lemon essential oil (LEO) and LEO microcapsules covered with mesquite gum – chia mucilage (MG-CM) mixtures and MG, stored during seven weeks, at 35 °C. Average values are shown (n = 3).

### 3.2.3. Oil oxidation kinetics

Fig. 5 shows the oxidation kinetics of LEO and LEO microcapsules covered with MG-CM mixtures and MG, stored at 35 °C per seven weeks. The initial hydroperoxides (HP) content of non-encapsulated LEO was of  $9.3 \pm 1.9$  meq HP kg<sup>-1</sup> of oil, which was rapidly oxidized during the first week of storage ( $183.3 \pm 8.5$  meq HP kg<sup>-1</sup> of oil); oxidation continued until reaching a very high peroxide value of  $351.2 \pm 11.3$  meq HP kg<sup>-1</sup> of oil at the fifth week of storage. Microencapsulation of LEO reduced its oxidation significantly, but the wall material composition affected the level of protection against oxidation. 90–10 and 80–10 MG-CM microcapsules provided a greater protection against LEO oxidation during storage than MG microcapsules, but the mixtures showed no significant ( $p > .05$ ) difference between them, indicative that CM contributed to reduce oxidation, but the oil oxidative stability was not dependent on its concentration.

LEO covered with 90–10 and 80–20 MG-CM mixtures and MG had their peroxide values peaks (maximum HP concentration) at second (91.6 and 90.5 meq HP kg<sup>-1</sup> of oil) and third (203.3 meq HP kg<sup>-1</sup> of oil) week of storage, respectively. At longer storage times, the peroxide value decreased continuously because the hydroperoxides reacted to form secondary lipid oxidation products (carbonyls and aldehydes) (Timilsena, Adhikari, Barrow, et al., 2016). Cortés-Camargo et al. (2017) showed a similar trend in the oxidation kinetics of micro-encapsulated LEO covered with MG – nopal mucilage mixtures stored under the same conditions of this study.

CM addition produced thicker biopolymer matrices evidenced by the larger particle size of the MG-CM microcapsules compared to that of MG, and afforded a greater protection to the encapsulated LEO, since the surface area to volume ratio and the contact area of the oil with oxygen were reduced (Soottitawat et al., 2005). However, CM addition in 90–10 and 80–20 MG-CM microcapsules was not enough to maintain the initial oxidation level during storage, and this could be related with the “shrinkage” that tends to damage the microcapsule

**Table 4**  
Zero-order kinetic parameters of LEO and LEO microcapsules covered with MG-CM and MG.

	Kinetic model $C_{HP} = K_{HP}t + C_{HP_0}$	$K_{HP}$ (meq hydroperoxides/kg of oil-day)	$r^2$
LEO	$C_{HP} = 11.81 t + 12.95$	$11.81 \pm 0.18^a$	0.94
LEO/90-10 MG-CM	$C_{HP} = 6.19 t + 12.74$	$6.19 \pm 0.35^c$	0.94
LEO/80-20 MG-CM	$C_{HP} = 6.12 t + 7.93$	$6.12 \pm 0.32^c$	0.99
LEO/MG	$C_{HP} = 10.17 t + 8.90$	$10.17 \pm 0.34^b$	0.94

Data are presented as means  $\pm$  SD (n = 3).

Values with different letters in the same column indicate significant difference ( $p \leq .05$ ).

LEO: lemon essential oil; MG: mesquite gum; CM: chia mucilage;  $C_{HP_0}$ : initial peroxide value at time zero;  $C_{HP}$ : peroxide value after time (t);  $K_{HP}$ : hydroperoxides formation rate constant;  $r^2$ : coefficient of linear determination.

**Table 5**  
Kinetic release parameters of LEO microcapsules covered with MG-CM and MG at different pH and temperature conditions.

pH = 2.5, 37 °C			
Mathematical model	90-10 MG-CM	80-20 MG-CM	MG
Zero order	$Q = 7.27 t + 20.22$ ( $r^2 = 0.77$ )	$Q = 2.32 t + 24.46$ ( $r^2 = 0.76$ )	$Q = 15.41 t + 24.18$ ( $r^2 = 0.79$ )
First order	$\ln(Q-100) = -0.41 t + 4.79$ ( $r^2 = 0.98$ )	$\ln(Q-100) = -0.09 t + 4.62$ ( $r^2 = 0.99$ )	$\ln(Q-100) = -0.77 t + 4.78$ ( $r^2 = 0.98$ )
Higuchi	$Q = 31.37 t^{1/2} - 3.66$ ( $r^2 = 0.91$ )	$Q = 17.68 t^{1/2} - 1.82$ ( $r^2 = 0.94$ )	$Q = 43.07 t^{1/2} + 3.75$ ( $r^2 = 0.97$ )
Peppas	$\ln Q = 0.75 \ln t + 2.90$ ( $r^2 = 0.90$ )	$\ln Q = 0.75 \ln t + 2.17$ ( $r^2 = 0.93$ )	$\ln Q = 0.46 \ln t + 3.87$ ( $r^2 = 0.94$ )
pH = 2.5, 65 °C			
Mathematical model	90-10 MG-CM	80-20 MG-CM	MG
Zero order	$Q = 9.09 t + 20.93$ ( $r^2 = 0.85$ )	$Q = 8.22 t + 20.29$ ( $r^2 = 0.82$ )	$Q = 13.31 t + 4.09$ ( $r^2 = 0.97$ )
First order	$\ln(Q-100) = -0.3 t + 4.56$ ( $r^2 = 1.0$ )	$\ln(Q-100) = -0.42 t + 4.82$ ( $r^2 = 0.98$ )	$\ln(Q-100) = -0.45 t + 5.03$ ( $r^2 = 0.89$ )
Higuchi	$Q = 32.56 t^{1/2} + 1.4$ ( $r^2 = 0.98$ )	$Q = 32.4 t^{1/2} - 1.82$ ( $r^2 = 0.95$ )	$Q = 39.76 t^{1/2} - 14.07$ ( $r^2 = 0.93$ )
Peppas	$\ln Q = 0.51 \ln t + 3.49$ ( $r^2 = 0.97$ )	$\ln Q = 0.66 \ln t + 3.16$ ( $r^2 = 0.91$ )	$\ln Q = 0.94 \ln t + 2.77$ ( $r^2 = 0.99$ )
pH = 6.5, 37 °C			
Mathematical model	90-10 MG-CM	80-20 MG-CM	MG
Zero order	$Q = 1.11 t + 55.97$ ( $r^2 = 0.35$ )	$Q = 1.6 t + 34.68$ ( $r^2 = 0.66$ )	$Q = 15.33 t + 7.71$ ( $r^2 = 0.93$ )
First order	$\ln(Q-100) = -0.09 t + 3.79$ ( $r^2 = 0.84$ )	$\ln(Q-100) = -0.13 t + 4.83$ ( $r^2 = 0.82$ )	$\ln(Q-100) = -0.61 t + 5.05$ ( $r^2 = 0.93$ )
Higuchi	$Q = 11.62 t^{1/2} + 34.11$ ( $r^2 = 0.64$ )	$Q = 14.87 t^{1/2} + 8.08$ ( $r^2 = 0.90$ )	$Q = 43.28 t^{1/2} - 11.55$ ( $r^2 = 0.93$ )
Peppas	$\ln Q = 0.31 \ln t + 3.6$ ( $r^2 = 0.69$ )	$\ln Q = 0.53 \ln t + 2.77$ ( $r^2 = 0.94$ )	$\ln Q = 0.95 \ln t + 2.95$ ( $r^2 = 0.95$ )
pH = 6.5, 65 °C			
Mathematical model	90-10 MG-CM	80-20 MG-CM	MG
Zero order	$Q = 2.2 t + 28.4$ ( $r^2 = 0.73$ )	$Q = 1.46 t + 37.08$ ( $r^2 = 0.6$ )	$Q = 14.36 t + 18.15$ ( $r^2 = 0.84$ )
First order	$\ln(Q-100) = -0.08 t + 4.49$ ( $r^2 = 0.98$ )	$\ln(Q-100) = -0.06 t + 4.3$ ( $r^2 = 0.92$ )	$\ln(Q-100) = -0.88 t + 5.2$ ( $r^2 = 0.93$ )
Higuchi	$Q = 17.02 t^{1/2} + 2.63$ ( $r^2 = 0.93$ )	$Q = 13.95 t^{1/2} + 11.49$ ( $r^2 = 0.86$ )	$Q = 42.54 t^{1/2} - 3.26$ ( $r^2 = 0.95$ )
Peppas	$\ln Q = 0.63 \ln t + 2.54$ ( $r^2 = 0.93$ )	$\ln Q = 0.58 \ln t + 2.63$ ( $r^2 = 0.84$ )	$\ln Q = 0.68 \ln t + 3.45$ ( $r^2 = 0.92$ )

LEO: Lemon essential oil; MG: Mesquite gum; CM: Chia mucilage; Q: cumulative percentage of released LEO; t: time;  $r^2$ : coefficient of linear determination.

surface favoring oxygen permeability (Bae & Lee, 2008).

On the other hand, MG microcapsules had smaller particle size, with greater surface area to volume ratio, which promoted oxidation (Jafari et al., 2008). MG has a branched compact spherical structure which diffuses rapidly to the oil-water interface during the emulsion formation (Vernon-Carter et al., 2000) and when it is spray-dried, it creates thin films which makes the oil closer to the surface facilitating its reaction with external oxygen (Soottitantawat et al., 2005).

The HP formation kinetics (Fig. 5) were tested using zero-order and first-order models finding that all the systems showed a better fit to zero-order kinetics ( $r^2 \geq 0.94$ ) until reaching their maximum HP concentration over the time. In shelf-life studies, zero-order reactions form a straight line by plotting a quality factor (positive or negative) versus time, and are independent of the reagent concentration (Han, 2005), i.e. the rate of HP formation was constant over the time and independent of the concentration of oil that was reacting. Table 4 shows the zero-order kinetic parameters of LEO and microencapsulated LEO covered with MG-CM and MG. Greater rate constants of HP formation ( $K_{HP}$ ) indicate a higher oxygen diffusion through the biopolymer matrix (Escalona-García et al., 2016). The  $K_{HP}$  of non-encapsulated LEO ( $11.81 \pm 0.18$  meq HP  $\text{kg}^{-1}$  of oil-day) was significantly ( $p \leq .05$ )

higher than that of microencapsulated LEO covered with MG ( $10.17 \pm 0.34$  meq HP  $\text{kg}^{-1}$  of oil-day) and both of them were significantly higher (approximately two-fold times) than  $K_{HP}$  of microencapsulated LEO covered with 90-10 and 80-20 MG-CM mixtures ( $6.19 \pm 0.35$  and  $6.12 \pm 0.32$  meq HP  $\text{kg}^{-1}$  of oil-day, respectively), indicating that MG-CM microcapsules achieved greater protection of LEO against oxidation. Soottitantawat et al. (2004) and Escalona-García et al. (2016) also found zero-order reactions in the oxidation kinetics of encapsulated oil using d-limonene and chia seed oil, respectively as core materials.

### 3.2.4. Oil release kinetics

Release kinetics of LEO encapsulated with MG-CM mixtures and MG were carried out under different pH and temperature conditions simulating the physicochemical conditions of food processing within the gastrointestinal tract, i.e. pH of 2.5 and 6.5, at two temperatures 37 °C (human body temperature) and 65 °C (food processing temperature) (Dima et al., 2016). The oil release kinetics data were tested using zero-order, first-order, Higuchi and Peppas models (Table 5).

Fig. 6a shows the release rate of LEO encapsulated with MG-CM and MG at pH = 2.5 and 37 °C. LEO release rate was faster in MG

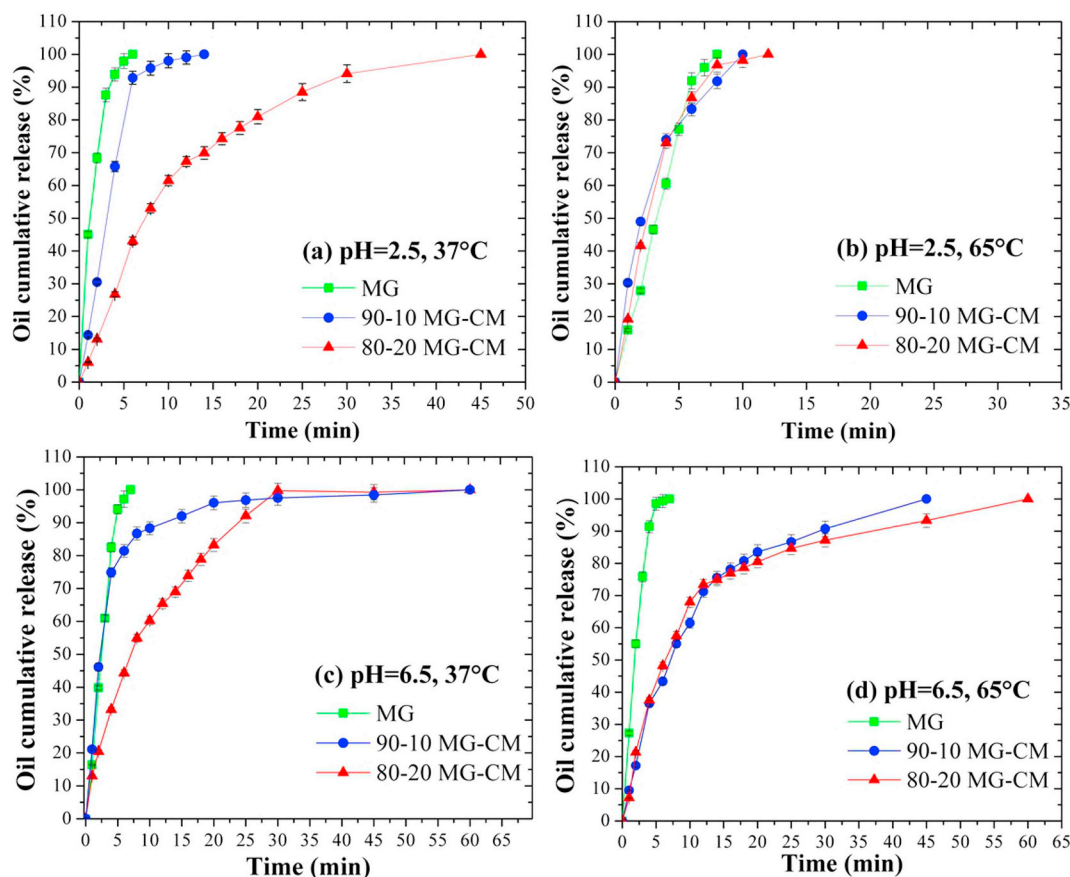


Fig. 6. Release kinetics of lemon essential oil encapsulated with mesquite gum – chia mucilage (MG-CM) mixtures and MG, using different conditions of pH (2.5 and 6.5) and temperature (37 °C and 65 °C). Average values are shown ( $n = 3$ ).

microcapsules, followed by 90–10 and 80–20 MG-CM microcapsules and there was significant difference between them ( $p \leq .05$ ). The three curves of oil release rate had the best fit to the first-order model ( $r^2 \geq 0.98$ ). Peppas equation allowed to determine the diffusion exponent “ $n$ ” of microcapsules which classifies the release mechanisms as follows:  $n \leq 0.43$  Fickian diffusion (case I transport);  $0.43 < n < 0.85$  anomalous or non-Fickian transport;  $n = 0.85$  zero-order release kinetic (case II transport) (Dima et al., 2016; Siepmann & Peppas, 2001) and  $n > 0.89$  “supra II” type transport (Dash, Narasimha-Murthy, Nath, & Chowdhury, 2010). In this case, the three microcapsules systems had a non-Fickian transport mechanism where the oil release is controlled by the biopolymer swelling and oil diffusion through the biopolymer matrix (Maderuelo, Zarzuelo, & Lanao, 2011).

Fig. 6b shows the release rate of LEO encapsulated with MG-CM and MG at pH = 2.5 and 65 °C. Under these conditions, the oil release rate was very fast since it occurred in a maximum time of 10 min and the type of wall material had not an effect on the oil release rates. The model that best described LEO release rate of 90–10 and 80–20 MG-CM microcapsules was the first-order model ( $r^2 \geq 0.98$ ) and of MG microcapsules was that of Peppas ( $r^2 = 0.99$ ). The transport mechanism of LEO encapsulated with 90–10 and 80–20 MG-CM was non-Fickian, and of LEO encapsulated with MG was “supra II” type transport which releases the oil by biopolymer erosion or degradation in contact with the dissolution medium (Dash et al., 2010; Maderuelo et al., 2011).

Fig. 6c shows the release rate of LEO encapsulated with MG-CM and MG at pH = 6.5 and 37 °C. Oil release rate was faster using MG microcapsules, followed by 90–10 and 80–20 MG-CM microcapsules. 90–10 and 80–20 MG-CM mixtures had different oil release rates but were not significantly different ( $p > .05$ ) in the range of 25 to 60 min. The model that best described the oil release rate of 80–20 MG-CM and MG microcapsules was that of Peppas ( $r^2 \geq 0.94$ ), and of 90–10 MG-CM

microcapsules was the first-order model ( $r^2 = 0.84$ ). The transport mechanism of LEO encapsulated with 80–20 MG-CM was non-Fickian, of LEO encapsulated with MG was “supra II” type transport and of LEO encapsulated with 90–10 MG-CM was Fickian where the oil release rate is only controlled by the diffusion process (Dima et al., 2016).

Fig. 6d shows the release rate of LEO encapsulated with MG-CM and MG at pH = 6.5 and 65 °C. Oil release rate was faster using MG microcapsules, followed by 90–10 and 80–20 MG-CM microcapsules and these mixtures had no significant difference ( $p > .05$ ) between them in most of the time studied. The model that best described the oil release rate of 90–10 MG-CM ( $r^2 = 0.98$ ) and 80–20 MG-CM microcapsules ( $r^2 = 0.92$ ) was the first-order model and of MG microcapsules was that of Higuchi ( $r^2 = 0.95$ ). All three LEO microcapsules systems had a non-Fickian transport mechanism.

Addition of CM in MG-CM microcapsules decreased the LEO release rate. The higher CM concentration in MG-CM microcapsules, the slower was the oil release rate. Oil release rate in MG-CM microcapsules was controlled by the swelling and the formation of a robust gel layer, decreasing the porosity of the wall material and the oil release rate. The acidic condition of the medium (pH = 2.5) favored the rapid oil release from microcapsules. Acidic conditions tend to produce the depolarization or reduction of the negative charge of the biopolymers, which reduces the viscosity and the resistance of gel (Maderuelo et al., 2011).

MG microcapsules showed the “burst effect” where a considerable percentage of oil is released in a relatively short period of time in contact with water (Maderuelo et al., 2011). The burst effect is attributed to oil molecules adsorbed on the microcapsules surface, that is, the biopolymer dissolution rate near to the surface is high, thus the amount of oil released is also high (Hosseini, Zandi, Rezaei, & Farahmandghavi, 2013). In this work, burst effect of MG microcapsules was attributed to



their small particle sizes and to their thin biopolymer matrices. The addition of CM in MG-CM microcapsules allowed to delay the LEO release rate avoiding the representative burst effect of MG microcapsules, besides it could be useful in the sensorial aspect, since CM addition could prolong the release and perception of lemon flavor in the mouth. On the other hand, the rapid LEO release from MG microcapsules could be exploited in the preparation of powdered instant beverages since these microcapsules are rapidly solubilized in water allowing the immediate release of the flavoring agent. Thus, depending on the application, the most convenient biopolymer matrix must be selected to control the oil release rate.

#### 4. Conclusions

MG-CM microcapsules in 90–10 and 80–20 ratios provided better protection to LEO against oxidation than MG microcapsules. The higher protection against LEO oxidation by the MG-CM mixtures was related with their emulsion and microcapsules characteristics, i.e. MG-CM emulsions had larger droplet sizes and higher apparent viscosity values than MG emulsion, and after being spray-dried, MG-CM microcapsules had larger particle sizes and smaller superficial area in contact with oxygen than MG microcapsules. The three microcapsules systems had low volatile oil retention values ( $\leq 51.5\%$ ) and high encapsulation efficiency values ( $\geq 96.9\%$ ). Furthermore, CM addition in MG-CM microcapsules contributed to delay the LEO release rate. A higher concentration of CM in MG-CM microcapsules led to a reduction in oil release rate due to the increase in the particle size and to the swelling and the formation of a robust gel layer around the microcapsules in contact with water. In contrast, MG microcapsules eroded in contact with water which led to a rapid oil release by burst effect. Studies of oil release kinetics should be considered for future applications of the encapsulated oil since they could have an effect on their functional and sensory characteristics. Finally, CM is an unexploited additive capable of interacting with MG for oil microencapsulation by spray drying, since these mixtures contributed to the improvement of the oxidative stability and to delay of the release rate of encapsulated LEO. In this way, MG-CM mixtures are interesting additives system suitable for being applied in food industry.

#### Conflict of interest

The authors declare no conflict of interest.

#### Acknowledgments

The authors wish to thank the financial support provided to the author Cortés-Camargo who receives a scholarship through the Consejo Nacional de Ciencia y Tecnología (CONACYT) of Mexico.

#### References

Bae, E. K., & Lee, S. J. (2008). Microencapsulation of avocado oil by spray drying using whey protein and maltodextrin. *Journal of Microencapsulation*, 25(8), 549–560.

Bringas-Lantigua, M., Expósito-Molina, I., Reineccius, G. A., López-Hernández, O., & Pino, J. A. (2011). Influence of spray-dryer air temperatures on encapsulated mandarin oil. *Drying Technology*, 29, 520–526.

Capitani, M. I., Ixtaina, V. Y., Nolasco, M. S., & Tomás, M. C. (2013). Microstructure, chemical composition and mucilage exudation of chia (*Salvia hispanica* L.) nutlets from Argentina. *Journal of the Science of Food and Agriculture*, 93(15), 3856–3862.

Capitani, M. I., Matus-Basto, A., Ruiz-Ruiz, J. C., Santiago-García, J. L., Betancur-Ancona, D. A., Nolasco, S. M., ... Segura-Campos, M. R. (2016). Characterization of biodegradable films based on *Salvia hispanica* L. protein and mucilage. *Food and Bioprocess Technology*, 9, 1276–1286.

Carneiro, H. C. F., Tonon, R. V., Grosso, C. R. F., & Hubinger, M. D. (2013). Encapsulation efficiency and oxidative stability of flaxseed oil microencapsulated by spray drying using different combinations of wall materials. *Journal of Food Engineering*, 115, 443–451.

Cervantes-Martínez, C. V., Medina-Torres, L., González-Laredo, R. F., Calderas, F., Sánchez-Olivares, G., Herrera-Valencia, E. E., ... Rodríguez-Ramírez, J. (2014). Study of spray drying of the *Aloe vera* mucilage (*Aloe vera barbadensis* Miller) as a function

of its rheological properties. *LWT - Food Science and Technology*, 55, 426–435.

Cortés-Camargo, S., Cruz-Olivares, J. E., Barragán-Huerta, B., Dublán-García, O., Román-Guerrero, A., & Pérez-Alonso, C. (2017). Microencapsulation by spray drying of lemon essential oil: Evaluation of mixtures of mesquite gum – nopal mucilage as new wall materials. *Journal of Microencapsulation*, 34(4), 395–407.

Cross, M. M. (1965). Rheology of non Newtonian fluids: A new flow equation for pseudoplastic systems. *Journal of Colloid Science*, 20, 417–437.

Dash, S., Narasimha-Murthy, P., Nath, L., & Chowdhury, P. (2010). Kinetic modeling on drug release from controlled drug delivery systems. *Acta Poloniae Pharmaceutica*, 67(3), 217–223.

De Campo, C., Pereira Dos Santos, P., Hass-Costa, T. M., Paese, K., Stanisquaski-Guterres, S., de Oliveira-Rios, A., & Hickmann-Flôres, S. (2017). Nanoencapsulation of chia seed oil with chia mucilage (*Salvia hispanica* L.) as wall material: Characterization and stability evaluation. *Food Chemistry*, 234, 1–9.

Dick, M., Hass-Costa, T. M., Gomaa, A., Subirade, M., de Oliveira-Rios, A., & Hickmann-Flôres, S. (2015). Edible film production from chia seed mucilage: Effect of glycerol concentration on its physicochemical and mechanical properties. *Carbohydrate Polymers*, 130, 198–205.

Dima, C., Pătrașcu, L., Cantaragiu, A., Alexe, P., & Ștefan, D. (2016). The kinetics of the swelling process and the release mechanisms of *Coriandrum sativum* L. essential oil from chitosan/alginate/inulin microcapsules. *Food Chemistry*, 195, 39–48.

Escalona-García, L. A., Pedroza-Islas, R., Natividad, R., Rodríguez-Huezo, M. E., Carrillo-Navas, H., & Pérez-Alonso, C. (2016). Oxidation kinetics and thermodynamic analysis of chia oil microencapsulated in a whey protein concentrate-polysaccharide matrix. *Journal of Food Engineering*, 175, 93–103.

Fuentes-Ortega, T., Martínez-Vargas, S. L., Cortés-Camargo, S., Guadarrama-Lezama, A. Y., Gallardo-Rivera, R., Baeza-Jiménez, R., & Pérez-Alonso, C. (2017). Effects of the process variables of microencapsulation sesame oil (*Sesamum indicum* L.) by spray drying. *Revista Mexicana de Ingeniería Química*, 16(2), 477–490.

García, M. C., Alfaro, M. C., Calero, N., & Muñoz, J. (2014). Influence of polysaccharides on the rheology and stabilization of  $\alpha$ -pinene emulsions. *Carbohydrate Polymers*, 105, 177–183.

García-Cruz, E. E., Rodríguez-Ramírez, J., Méndez-Lagunas, L. L., & Medina-Torres, L. (2013). Rheological and physical properties of spray-dried mucilage obtained from *Hylocereus undatus* cladodes. *Carbohydrate Polymers*, 91(1), 394–402.

Goh, K. K. T., Matia-Merino, L., Chiang, J. H., Quek, R., Soh, S. J. B., & Lentle, R. G. (2016). The physico-chemical properties of chia seed polysaccharide and its microgel dispersion rheology. *Carbohydrate Polymers*, 149, 297–307.

Guiotto, E. N., Capitani, M. I., Nolasco, S. M., & Tomás, M. C. (2016). Stability of oil-in-water emulsions with sunflower (*Helianthus annuus* L.) and chia (*Salvia hispanica* L.) by-products. *JAOCs Journal of the American Oil Chemists' Society*, 93, 133–143.

Han, J. H. (2005). *Innovations in food packaging* (1st ed.). Oxford, UK: Elsevier Academic Press.

Hosseini, S. F., Zandi, M., Rezaei, M., & Farahmandghavi, F. (2013). Two-step method for encapsulation of oregano essential oil in chitosan nanoparticles: Preparation, characterization and *in vitro* release study. *Carbohydrate Polymers*, 95(1), 50–56.

Jafari, S. M., Assadpoor, E., He, Y., & Bhandari, B. (2008). Encapsulation efficiency of food flavours and oils during spray drying. *Drying Technology*, 26, 816–835.

Kaewmanee, T., Bagnasco, L., Benjakul, S., Lanteri, S., Morelli, C. F., Speranza, G., & Cosulich, M. E. (2014). Characterisation of mucilages extracted from seven Italian cultivars of flax. *Food Chemistry*, 148, 60–69.

Labuza, T. P. (1984). Application of chemical kinetics to deterioration of foods. *Journal of Chemical Education*, 61(4), 348–358.

Lin, K. Y., Daniel, J. R., & Whistler, R. L. (1994). Structure of chia seed polysaccharide exudate. *Carbohydrate Polymers*, 23, 13–18.

Lopes Da Silva, J. A., Gonçalves, M. P., & Rao, M. A. (1992). Rheological properties of high-methoxyl pectin and locust bean gum solutions in steady shear. *Journal of Food Science*, 57(2), 443–448.

Maderuelo, C., Zarzuelo, A., & Lanao, J. M. (2011). Critical factors in the release of drugs from sustained release hydrophilic matrices. *Journal of Controlled Release*, 154(1), 2–19.

Muñoz, L. A., Cobos, A., Diaz, O., & Aguilera, J. M. (2012). Chia seeds: Microstructure, mucilage extraction and hydration. *Journal of Food Engineering*, 108(1), 216–224.

Niu, F., Niu, D., Zhang, H., Chang, C., Gu, L., Su, Y., & Yang, Y. (2016). Ovalbumin/gum arabic-stabilized emulsion: Rheology, emulsion characteristics, and Raman spectroscopic study. *Food Hydrocolloids*, 52, 607–614.

Piorkowski, D. T., & McClements, D. J. (2014). Beverage emulsions: Recent developments in formulation, production, and applications. *Food Hydrocolloids*, 42, 5–41.

Rodea-González, D. A., Cruz-Olivares, J., Román-Guerrero, A., Rodríguez-Huezo, M. E., Vernon-Carter, E. J., & Pérez-Alonso, C. (2012). Spray-dried encapsulation of chia essential oil (*Salvia hispanica* L.) in whey protein concentrate-polysaccharide matrices. *Journal of Food Engineering*, 111, 102–109.

Segura-Campos, M. R., Ciau-Solis, N., Rosado-Rubio, G., Chel-Guerrero, L., & Betancur-Ancona, D. (2014). Chemical and functional properties of chia seed (*Salvia hispanica* L.) gum. *International Journal of Food Science*, 2014, 1–5.

Shantha, N. C., & Decker, E. A. (1994). Rapid, sensitive, iron-based spectrophotometric methods for determination of peroxide values of food lipids. *Journal of AOAC International*, 77(2), 421–424.

Siepmann, J., & Peppas, N. A. (2001). Modeling of drug release from delivery systems based on hydroxypropyl methylcellulose (HPMC). *Advanced Drug Delivery Reviews*, 48, 139–157.

Sittikijyothin, W., Torres, D., & Gonçalves, M. P. (2005). Modelling the rheological behaviour of galactomannan aqueous solutions. *Carbohydrate Polymers*, 59, 339–350.

Soottinantawat, A., Bigeard, F., Yoshii, H., Furuta, T., Ohkawara, M., & Linko, P. (2005). Influence of emulsion and powder size on the stability of encapsulated  $\alpha$ -limonene by spray drying. *Innovative Food Science and Emerging Technologies*, 6(1), 107–114.

- Soottitantawat, A., Yoshii, H., Furuta, T., Ohgawara, M., Forssell, P., Partanen, R., ... Linko, P. (2004). Effect of water activity on the release characteristics and oxidative stability of D-limonene encapsulated by spray drying. *Journal of Agricultural and Food Chemistry*, *52*(5), 1269–1276.
- Steffe, J. F. (1996). *Rheological methods in food process engineering* (2nd ed.). East Lansing, MI, USA: Freeman Press.
- Tan, L. H., Chan, L. W., & Heng, P. W. S. (2009). Alginate/starch composites as wall material to achieve microencapsulation with high oil loading. *Journal of Microencapsulation*, *26*(3), 263–271.
- Timilsena, Y. P., Adhikari, R., Barrow, C. J., & Adhikari, B. (2016). Microencapsulation of chia seed oil using chia seed protein isolate-chia seed gum complex coacervates. *International Journal of Biological Macromolecules*, *91*, 347–357.
- Timilsena, Y. P., Adhikari, R., Kasapis, S., & Adhikari, B. (2016). Molecular and functional characteristics of purified gum from Australian chia seeds. *Carbohydrate Polymers*, *136*, 128–136.
- Tonon, R. V., Grosso, C. R. F., & Hubinger, M. D. (2011). Influence of emulsion composition and inlet air temperature on the microencapsulation of flaxseed oil by spray drying. *Food Research International*, *44*(1), 282–289.
- Tonon, R. V., Pedro, R. B., Grosso, C. R. F., & Hubinger, M. D. (2012). Microencapsulation of flaxseed oil by spray drying: Effect of oil load and type of wall material. *Drying Technology*, *30*, 1491–1501.
- Utrilla-Coello, R. G., Hernández-Jaimes, C., Carrillo-Navas, H., González, F., Rodríguez, E., Bello-Pérez, L. A., ... Alvarez-Ramírez, J. (2014). Acid hydrolysis of native corn starch: Morphology, crystallinity, rheological and thermal properties. *Carbohydrate Polymers*, *103*, 596–602.
- Velázquez-Gutiérrez, S. K., Figueira, A. C., Rodríguez-Huezo, M. E., Román-Guerrero, A., Carrillo-Navas, H., & Pérez-Alonso, C. (2015). Sorption isotherms, thermodynamic properties and glass transition temperature of mucilage extracted from chia seeds (*Salvia hispanica* L.). *Carbohydrate Polymers*, *121*, 411–419.
- Vernon-Carter, E. J., Beristain, C. I., & Pedroza-Lslas, R. (2000). Mesquite gum (*Prosopis* gum). In G. Doxastakis, & V. Kiosseoglou (Eds.). *Novel macromolecules in food systems* (pp. 217–238). Amsterdam, Netherlands: Elsevier.
- Vernon-Carter, E. J., Gómez, S. A., Beristain, C. I., Mosqueira, G., Pedroza-Islas, R., & Moreno-Terrazas, R. C. (1996). Color degradation and coalescence kinetics of Azte marigold oleoresin-in-water emulsions stabilized by mesquite or arabic gums and their blends. *Journal of Texture Studies*, *27*(6), 625–641.